Ocean Sci. Discuss., 5, 507–543, 2008
www.ocean-sci-discuss.net/5/507/2008/

Ocean Science
Discussions

Papers published in *Ocean Science Discussions* are under
open-access review for the journal *Ocean Science*

Role of cabbeling in water densification in the Greenland Basin

Y. Kasajima[1] and T. Johannessen[1,2]

[1]Geophysical Institute, University of Bergen. Allégaten 70, 5007 Bergen, Norway
[2]Bjerkrnes Centre for Climate Research, Allégaten 55, 5007 Bergen, Norway

Received: 22 July 2008 – Accepted: 26 August 2008 – Published: 12 September 2008

Correspondence to: Y. Kasajima (yoshie.kasajima@gfi.uib.no)

Published by Copernicus Publications on behalf of the European Geosciences Union.

Abstract

The contribution of cabbeling mixing to water mass modification in the Greenland Sea was explored from hydrographic observation across the Greenland Basin in summer 2006. Neutral surface was chosen as a reference frame, and the strength of cabbeling mixing was determined by the dianeutral velocity magnitude. Water types in the area were classified into North Atlantic Water (NAW), modified North Atlantic Water (mNAW), water from Barents Sea near Bear Island (BIW), Arctic Intermediate Water (AIW) and Deep Water (DW), and significant cabbeling-induced velocity (>1 m/day) appeared at the interfaces of these water types below the seasonal pycnocline. The mixing between BIW and NAW in the eastern periphery was the most vigorous, where mixing-induced velocity reached 7.5 m/day which accompanied NAW production of 123 m^3/day through transformation of BIW. Cabbeling in the Arctic Frontal Zone was found of two types; mixing within NAW in the upper layer and mixing within mNAW in the lower layer with a maximum velocity of 3 m/day. Source waters in the central Greenland Basin were AIW and mNAW and produced a vertical velocity of 4 m/day. In the western part of the Greenland Basin, the areas of active cabbeling were widely separated and each mixing point appeared rather weak, with a maximum velocity of 2.5 m/day. The average density gain in the eastern periphery was 0.003 kg/m^3 while it was 0.001 kg/m^3 in the other areas, though the impact of cabbeling on the bulk buoyancy change was highest in the western Greenland Sea. The frontal areas occupied approximately 50% of the whole analysis area and the total density gain due to cabbeling mixing in the Greenland Basin as a whole was estimated as 6.7×10^{-4} kg/m^3.

1 Introduction

Inter-basin density variation induces water movement from denser to lighter water, and this buoyancy-induced current contributes to the global ocean circulation together with wind-driven currents in the upper layer. Although the global relation between upper and lower currents is not clear, changes in lower layer circulation can influence the upper layer circulation, therefore the investigation of buoyancy-induced currents is important in a climatological aspect. In the northern Atlantic sector, the water in the Greenland-Iceland-Norwegian (GIN) seas is denser than that in the North Atlantic Ocean, and the denser water in the GIN Sea flows out to the North Atlantic, which is distinguished as a meridional overturning current. The density contrast between the GIN Sea and the North Atlantic is owing to the hydrographic condition of the Greenland Sea, which allows deep water formation. The cyclonic gyre and winter surface cooling in the central Greenland Sea creates an ideal condition for Deep Convection and the interplay between warm saline North Atlantic inflow and cold less saline water outflow from the Arctic Ocean promotes the formation of Greenland Sea Deep Water. The observations of the last decades, however, indicate that Deep Convection in the central Greenland Sea has been weakened. Consequently, the dense water in the Greenland Basin has not been renewed and the temperature of the dense water has increased, which leads to a decrease of the water density (Clarke et al., 1990, Bönisch et al., 1997; Budéus et al., 1998; Jansen and Opheim, 1999; Karstensen et al., 2005). This implies less density contrast between the GIN Sea and North Atlantic, retarding the meridional circulation. Although the dense water in the GIN Sea is fundamental for the buoyancy-induced circulation, the direct contribution to the southward overflow is the intermediate water which is formed through shallow convection, subduction and gradual transformation of Atlantic Water (Hansen and Østerhus, 2000). The formation of intermediate water interacts with deep water property, and small scale mixing processes play an essential role in the modification of water properties in the whole basin. Small scale mixing is highly localised and the evaluation of its impacts on the global circulation is not an easy task. Nevertheless, it is important to investigate the effects of small scale mixing on water modification and subsequent change of the overall hydrographic condition, especially when deep convection weakens.

Mechanical turbulent mixing is generally the most robust mixing process. Its principal source is external forces such as wind and tides, and turbulence by wind and tides

OSD

5, 507–543, 2008

homogenises the upper layer. Wind- and tidal-induced internal waves are important agents for deep water modification by enhancing turbulent mixing in the ocean interior. The contribution of turbulent mixing to buoyancy change is represented in terms of the vertical diffusivity. Munk and Wunch (1998), however, found that turbulent mixing alone is not enough to balance the global upwelling and claimed that including all significant turbulent mixing spots in deep-ocean was required for a proper estimation of diffusivity. Further investigation of significant turbulent mixing spots in deep-oceans is necessary, though the insufficiency of turbulent mixing implies that the contribution of other mixing processes can be substantial in the basin scale change of buoyancy.

Apart from turbulent mixing, important small scale mixing processes include double diffusion, cabbeling and thermobaricity. The driving force of double diffusion is the difference in the molecular diffusivity of heat and salt. Temperature diffuses much faster than salt and thus a water parcel loses heat quickly while salinity remains unchanged, and the density of the water parcel changes without external forcing. Cabbeling and thermobaricity occur due to the nonlinear features of seawater. The first is a mixing of water masses with different properties, which produces water denser than source waters, and the second is the densification of a water parcel as a result of compressibility where cold water is more compressible than warm water. In high latitudes, the presence of sea ice cools surface waters nearly to the freezing point and can create a sharp interface in the surface layer between cold less saline water on top and warmer and saline water below. This is a prerequisite for double diffusive convection, and the strong stratification can cause an abrupt overturning through thermobaricity (Akitomo, 1999). In the Barents Sea, double diffusive mixing plays an important role when the shear-induced turbulent mixing is relatively weak (Sundfjord et al., 2007). At the Arctic Front to the west of Spitsbergen, warm and saline North Atlantic Water and cold and less saline Arctic Water create an ideal hydrographic condition for double diffusion and cabbeling processes (Cottier and Venables, 2007).

McDougall (1987a) derived a water mass modification equation for turbulent mixing, double diffusion, cabbeling and thermobaricity and estimated that cabbeling and thermobaric processes in the North Atlantic would cause water-mass conversion of a magnitude equal to that caused by a vertical diffusivity of 10^{-4} m^2 s^{-1}. A theoretical study by Garrett and Horne (1978) exhibited that cabbeling processes caused a significant sinking rate at fronts and may drive vertical circulations to maintain fronts against diffusion. Horne (1978) showed that cabbeling was the dominant mechanism which drove vertical circulation at the subsurface front between warm slope water and Labrador slope water, and You (1996) demonstrated that the contribution of cabbeling together with thermobaricity was significant for vertical transport in the Indian Ocean. At the Antarctic Polar Frontal Zone, cabbeling mixing plays an important role in a strong cross-frontal exchange (Gordon et al., 1977; You, 1999) and it also can cause a significant diapycnal volume flux (Marsh, 2000). In the western Pacific, cabbeling in combination with double diffusion is the major mechanism for water transformation in the subarctic front (Talley and Yun, 2001).

The purpose of the paper is to investigate the role of cabbeling in water densification in the Greenland Basin. In the following sections, we demonstrate hydrographic conditions and dominant water types in the Greenland Basin (Sect. 2) and review the water mass modification equation in neutral surface coordinates (Sect. 3). In the Sect. 4 the significant cabbeling mixing areas are determined from the cabbeling-induced vertical velocity and the water mass formation rate and densification of water associated with cabbeling mixing are estimated. The results are summarised in the Sect. 5.

2 Hydrography

In July 2006 hydrographic observations with water sampling for the chemical analysis were performed from R/V G.O.Sars under the EU-project CARBOOCEAN. The observations were carried out across the Greenland Basin with 34 CTD stations along 75° N in the central Greenland Sea and 24 CTD stations along 74.5° N on the basin slope towards Bear Island (Fig. 1).

CTD observations demonstrate the general hydrographic features in the Greenland

OSD
5, 507–543, 2008

Sea; warm Atlantic water flows northward on the east, cold less saline water in the central part, fresh water in the western surface layer and re-circulated Atlantic water below the fresh water (Fig. 2). The dominant water type on the east, North Atlantic Water (NAW), is found in the upper 500 m with salinity more than 35. Within the dominant NAW, two NAW cores (S>35.1), can be identified; one is around 16° E and another around 9° E and a cold water column around 10° E separates these two cores. Further west, there is another saline water column around 6° E and a saline water patch around 3° E, which is a forefront of NAW in the eastern Greenland Sea. The area with significant horizontal property gradients due to NAW is distinguished as the Arctic Frontal Zone. According to observations along 74.45° N in February 1989 there are four frontal interfaces in the Arctic Frontal Zone (van Aken et al. 1991). The locations of these fronts agree well with our observations, though our easternmost front is located around 10° E, slightly to the west of that obtained in 1989. These fronts are named front A, B, C and D following van Aken et al. (1991). On the western part, the re-circulated NAW extends vertically through about 400 m with the salinity of re-circulated NAW comparable to that of NAW on the east. Low salinity water in the surface layer is rather insignificant in 2006. On the easternmost part of the basin, there is another water type of less saline and cold water. It creates a sharp interface with NAW and can be identified as Spitsbergen Bank Water (SBW, Loeng, 1990). SBW is formed locally in the Barents Sea and the sharp interface with NAW can be the westward continuation of the front which is formed along Spitsbergen Bank.

The water masses in the Greenland and Iceland Seas were classified by Swift and Aagaard (1981) and they are listed in Table 1. The hydrographic data in 2006 are compared to their definitions on a T-S diagram (Fig. 3). The dataset in 2006 shows that Greenland Sea Deep Water (GSDW) is absent and that the densest water, which is less than σ_θ=28.1, is classified rather as Norwegian Sea Deep Water (NSDW). Polar Water (PW) is present but its amount is very small, instead, there is very low salinity water (<33.0). Salinity of Atlantic Water (AW) is more than 35.1 according to Swift and Aagaard (1981), though most of the NAW shown in Fig.2b tends to be less saline

OSD

5, 507–543, 2008

and colder. Variability of the North Atlantic Current can cause the change of local NAW properties, hence the different properties of NAW from those of AW given above can be the result of variability of the North Atlantic Current. Incidentally, van Aken et al. (1995) defined NAW with the properties of θ>3°C, S>35.0. SBW properties in 2006 are also different from the definition of Loeng (1990), having become slightly warmer and more saline.

The lack of GSDW and the discrepancy in water properties from the definition of Swift and Aagaard (1981) indicates that water properties in the Greenland Basin have changed through decades, therefore, we re-define water types as a matter of convenience based on the water types listed in Table 1. van Aken et al. (1995) defined waters of Atlantic origin as Atlantic Water type with S>34.9 and θ>2°C. The AW property can be applied to NAW in 2006, however, the salinity of re-circulated NAW on the west is as high as that of NAW in the east. In order to separate NAW from re-circulated NAW we define NAW to have S>34.9 and θ>3°C while the re-circulated NAW is colder than 3°C. According to this definition re-circulated NAW can include colder NAW in the eastern Greenland Sea, therefore this water type is called modified NAW (mNAW). The temperature and salinity ranges of SBW are expanded and the water is re-named as Bear Island Water (BIW). Water corresponding to NSDW property is re-named as Dense Water (DW). PW is very small in volume and hence is not considered in this study. The interior water in the Greenland Basin is classified as Arctic Intermediate Water (AIW), which is less saline than NAW and warmer than DW. These re-defined water properties are listed in Table 2 together with their volume percentages.

The re-defined water types occupy about 70% of the volume in the cross-section and the rest can be thought as a mixture of the defined waters. Within the defined water types, DW accounts for the largest part and the percentage of NAW, mNAW, AIW and BIW together is less than half of DW (about 16%). Even though the volume amount is minor, these water types are important source for heat and salt in the Greenland Basin and also for DW property change in the long term. The high density in Greenland Basin is due to the large volume of DW and about 30% of the total water volume, which is not classified into water types listed in Table 4, has low temperature with density close to DW. These dense waters determine the overall density of the Greenland Basin.

3 Water mass modification equation

The neutral surface, which is a surface satisfying the relation,

$$\alpha \nabla_n \theta = \beta \nabla_n S. \tag{1}$$

is used as the coordinate system in this study. α and β are thermal expansion and haline contraction coefficients defined as

$$\alpha = -\frac{1}{\rho}\frac{\partial \rho}{\partial \theta}\bigg|_{S,p} = \alpha' \left[\frac{\partial \theta}{\partial T}\bigg|_{S,p}\right]^{-1} \qquad \beta = -\frac{1}{\rho}\frac{\partial \rho}{\partial S}\bigg|_{\theta,p} = \beta' + \alpha\frac{\partial \theta}{\partial S}\bigg|_{T,p}$$

and ∇_n is the lateral gradient operator along a neutral surface (the definition of α' and β', see Gill, 1982). The neutral surface allows a water parcel to move without experiencing a buoyancy restoring force along the surface, whereas on an isopycnal surface the restoring force becomes significant with distance from the reference level due to the effect of compressibility. Therefore, the neutral surface frame is more appropriate for the study of the lateral mixing. In the analysis domain, neutral surfaces are calculated eastward from the points with certain density (σ_θ=27.50, 27.51, ... 28.07 with the interval of 0.01) in the westernmost station and 58 neutral surfaces (γ27.50, γ27.51, ..., γ28.07) are determined. When a neutral surface outcrops it cannot be traced further since the water properties are not conserved along a neutral surface. In the study area, γ27.50–γ27.55 outcrops already by 10.7° W, and γ27.56 by 2° W, therefore water properties below γ27.56 are analysed across the whole basin.

Selected neutral surfaces and their isopycnal counterparts, potential density referenced to surface, are shown in Fig. 4. The deviation between neutral surfaces and the isopycnals becomes notable with depth and tends to be larger toward the eastern periphery. Neutral surfaces appear shallower than isopycnals and the difference tends to be conspicuous in the middle of the Greenland Basin, in which $\gamma 28.07$ appears around 1500 m while σ_θ=28.07 appears at nearly 1800 m. The deeper location of isopycnals causes higher pressure gradients along the isopycnals that would lead to erroneous lateral mixing (McDougall, 1987b). The neutral layers above $\gamma 28.0$ are confined in shallow waters in the central Greenland Sea while layers from $\gamma 28.0$ to $\gamma 28.07$ occupy most of the spatial domain (100 m–1500 m). Along 74.5° N, the neutral surfaces are spaced more evenly and the vertical distance between $\gamma 28.0$ and $\gamma 28.07$ is decreased to 150 m in the eastern periphery. The thickness from $\gamma 28.0$ to $\gamma 28.07$ can be interpreted as the thickness of the intermediate water layer and $\gamma 28.07$ can correspond to the permanent pycnocline which separates the intermediate water from the deep water in the basin. The analysis domain in this study represents the surface and intermediate layers.

McDougall (1984, 1987a) formulated an equation of vertical velocity associated with turbulence, double diffusion, cabbeling and thermobaricity from the conservation equations for heat and salt. It is expressed as,

$$(e - D_z)\, g^{-1} N^2 = D\,(\alpha\theta_{zz} - \beta S_{zz}) + \left(\beta F_z^S - \alpha F_z^\theta\right) - \kappa\left[\theta_z C_{cb} \left|\nabla_n \theta\right|^2 + \theta_z C_{th} \nabla_n \theta \cdot \nabla_n p\right] \quad (2)$$

Here κ and D indicate the epineutral and dianeutral diffusion coefficients, $R_\rho=\alpha\theta_z/\beta S_z$ is a density ratio and F^θ, F^s are the double diffusive fluxes of heat and salinity.

C_{cb} and C_{th} are cabbeling and thermobaric parameters, expressed as

$$C_{cb}(\theta, S, p) = \left[\frac{\partial\alpha}{\partial\theta} + 2\frac{\alpha}{\beta}\frac{\partial\alpha}{\partial S} - \frac{\alpha^2}{\beta^2}\frac{\partial\beta}{\partial S}\right], \quad C_{th}(\theta, S, p) = \left[\frac{\partial\alpha}{\partial p} - \frac{\alpha}{\beta}\frac{\partial\beta}{\partial p}\right].$$

The terms on the right side of Eq. (2) indicate turbulent mixing, double diffusive mixing and non-linear processes (cabbeling and thermobaricity). The vertical velocity, e, is the result of these mixing processes and the velocity due to cabbeling process only is written as

$$e_{cb} = -g N^{-2} \kappa \left|\nabla_n \theta\right|^2 C_{cb}(\theta, S, p). \quad (3)$$

OSD

5, 507–543, 2008

Cabbeling in the Greenland Basin

Y. Kasajima and T. Johannessen

The cabbeling-induced velocity Eq. (3) is used for an indicator of the strength of cabbeling mixing. Prior to the quantitative study of cabbeling in the next section, the effective diffusivity due to cabbeling is calculated in order to see the significance of cabbeling in the study area. The effective diffusivity is equivalent to the vertical diffusivity that will cause the same vertical velocity calculated from Eq. (2), and it is (McDougall, 1987a)

$$D_{cb} = \kappa \left|\nabla_n \theta\right|^2 C_{cb}(\theta, S, p) \Big/ (\alpha\theta_{zz} - \beta S_{zz}). \qquad (4)$$

Using the lateral diffusivity κ=550 m^2 s^{-1} estimated from the tracer release experiment in the central Greenland Sea (Messias, et al., 2007), the effective diffusivity averaged over the whole Greenland Sea is $D_{cb}=3.4\times10^{-6}$ m^2/s. This is not very significant, however the spatial variation in the diffusivity is large and the maximum D_{cb} exceeds 0.1 m^2/s. It is expected that cabbeling mixing plays an important role in certain areas even though the space-average of cabbeling effects can be rather insignificant.

4 Cabbeling mixing in the Greenland Basin

4.1 Cabbeling-induced velocity

Cabbeling mixing is highly localised like other small scale mixing, and the effects of cabbeling are evaluated by exploring the active cabbeling spots. In order to identify the active cabbeling spots, dianeutral velocity is calculated from Eq. (3) and the result is shown in Fig. 5. High velocity patches appear intermittently in space and are absent in the vast area above γ27.7 in the western and central Greenland Sea, and below γ27.8 in the eastern periphery. The velocity patch in the eastern periphery, the highest over the whole area, appears as a columnar structure from near surface to bottom which corresponds to the interface between BIW and NAW. The velocity maxima in the water column are seen around γ27.65 with the highest magnitude of 7.5 m/day and another close to the bottom. In the Arctic Frontal Zone (2° E∼15° E) the high velocity patches, all lower than $\gamma 27.77$, appear around 10° E, 8° E, 6° E, consistent with the location of the four fronts (Sect. 2). The highest velocity is at front B (at 6° E) with a value of 3 m/day around $\gamma 28.0$. The velocity patch shifts position deeper towards the west, and it is seen at $\gamma 28.0$ with the magnitude of 4 m/day in the central basin. Further west, the high velocity patch is more widely spread over the area below $\gamma 28.0$, and the velocity is rather low with the maximum value less than 3 m/day. These patches of higher velocity in the central and western Greenland Basin correspond approximately to the interfaces with NAW and mNAW.

According to Horne and Garrett (1978) the typical cabbeling-induced vertical velocity at fronts is 1 m/day, and this value is used as the basis for significant cabbeling mixing. The locations of source waters which induce vertical velocities of more than 1m/day are shown in Fig. 6. Four areas with enhanced velocity are distinguished; near Bear Island, in the Arctic Frontal Zone, the central and the western Greenland Sea. These areas are recognised as frontal areas and are referred to as SB, AFZ, CG and WG, respectively (see Table 3 for details). From Fig. 4, the first three fronts are located in the surface layer or in the upper part of the intermediate layer, whereas mixing in WG arises in the intermediate layer and even at the lower edge of the intermediate layer.

The distribution of velocity patches can be partly explained by the velocity equation. The formula, Eq. (3), indicates that the cabbeling-induced velocity is a hyperbolic relation with respect to buoyancy frequency and a parabolic relation with respect to the temperature gradient. The buoyancy frequency across the Greenland Sea shows that the strongest stratification is found in the upper layer in the western part (Fig. 7). This is due to the influence of sea ice and the strong stratification prevents vertical velocity, which explains the lack of high velocity patches above $\gamma 27.7$ in the western part. The presence of sea ice creates a sharp lateral interface at the ice edge but does not induce significant vertical velocity. The buoyancy frequency and the lateral temperature gradient are competing factors, but high velocity (>1 m/day) appears only below the stratified layers. Below the stratified area, the contribution of temperature gradient to the velocity magnitude would be more important. The ratio of the temperature gradient

OSD
5, 507–543, 2008

Cabbeling in the Greenland Basin

Y. Kasajima and T. Johannessen

to buoyancy has a linear relation with the induced velocity (Fig. 8). The high ratio indicates high temperature gradient under low stratification and the linear relation between the lateral gradient to stratification ratio and velocity indicates that high velocity is owing to high temperature gradient.

In addition to stratification and the temperature gradient, the velocity is also dependent on cabbeling parameter. The relation between velocity and the cabbeling parameter exhibits that velocity maxima appear around 1.20×10^{-5} and 1.34×10^{-5} (Fig. 9). The cabbeling parameter is a second derivative of density with respect to temperature and salinity, and hence it can characterise the local hydrography. The eastern periphery is described by high temperature and relatively shallow water while temperature in the west is colder and water is deeper. The thermal expansion coefficient α decreases with temperature and increases with pressure, and the haline contraction coefficient β decreases with salinity and pressure. The eastern periphery is characterised by high α and low β, whereas the western area is characterised by low α and high β, and the cabbeling parameter is consistent with the α- and β-distributions (Fig. 10). Most of active cabbeling is found in high βregions whereas SB appears in high α regions where contours of the cabbeling parameters distribute vertically. The lateral change in the cabbeling parameter seems to be an important factor for the production of significant vertical velocities.

4.2 Water modification at frontal areas

Cabbeling forms water denser than its source waters, and produces changes in volume and in the thickness of layers. The volume change in certain layers can be quantified by the water mass formation rate defined by Walin (1982). He estimated the water formation rate in an isopycnal context whereas we use the neutral surface as a reference frame. The water formation rate, M through neutral surface coordinate γ, is expressed as

$$M(\gamma) = \partial G(\gamma)/\partial\gamma \tag{5}$$

OSD
5, 507–543, 2008

where G is the volume flux across γ. The positive (negative) formation rate indicates an increase (decrease) of the layer thickness, and the vertically integrated M indicates the change in the water volume due to cabbeling mixing in the column. Our observations are spatially limited and a precise volume transport per unit area cannot be obtained, therefore, the velocity averaged over the surface γ in each frontal area is assumed to represent the volume transport per unit area. The volume flux through the lowest neutral surface is calculated by assuming that the velocity at the layer below is zero. Figure 11 shows averaged velocity as a function of $\gamma$and the formation rate in each frontal area.

The velocity averaged over surfaces at fixed γ in SB increases from the surface to γ27.63, leading to a thinning of layers above γ27.63. The formation rate turns positive below the velocity maximum and produces 100~240 m^3/day of water in the range of γ27.63~γ27.66. The mixing source waters in SB are BIW and NAW or within NAW (Fig. 12a), and all resultant water is classified as NAW. This indicates that water produced in the range of γ27.63~γ27.66, considered to fall within NAW, has been either transformed from BIW or further densified NAW. In the deeper layers, the sign of the formation rate changes with velocity maxima and the highest formation rate in excess of 250 m^3/day is found in the lowest layer with γ27.77. The formation rate integrated through the whole SB is 123 m^3/day. This indicates that cabbeling transports surface waters downward by modifying BIW to NAW.

The mixing in AFZ is identified in two groups: mixing within NAW; and mixing within mNAW, or between AIW and mNAW (Fig. 12b). The first group (mixing within NAW) occurs in shallower layers between γ27.8 and γ27.9, which corresponds to the whole AFZc and the upper part of AFZb (see Table 3). The resultant newly formed NAW is denser than its source water NAW and accumulates in layers γ27.87~γ27.90 with the highest rate of 110 m^3/day at γ27.90. Although the overall formation rate in this group is very small (1.1×10^{-11} m^3/day), the sign of the formation rate is positive and hence a very small amount of NAW is produced within these layers. The second group (mixing between mNAW and AIW or within mNAW) appears lower than γ27.9 where the

OSD
5, 507–543, 2008
Cabbeling in the Greenland Basin
Y. Kasajima and T. Johannessen

mixing layers are divided into the ranges of $\gamma 27.93 \sim \gamma 27.94$ and $\gamma 27.98 \sim \gamma 28.0$. The formation rate at the bottom of these layers is more than 230 m^3/day, which is double that of NAW mixing layers above. The overall formation rate in this second group is negative (-1.2×10^{-10} m^3/day), and thus cabbeling transports a small amount of water to deeper layers. In AFZ, cabbeling mixing densifies NAW denser without changing the total volume, and hence it decreases the potential energy of the area.

The mixing in CG is enhanced around $\gamma 28.0$, where the water depth is shallower than 200 m and close to the upper boundary of the intermediate layer. The velocity averaged at γ is slightly lower than that in AFZ in the same layer levels. The mixing source waters are AIW and mNAW and the resultant water is mNAW (Fig. 12c). The formation rate changes according to the velocity magnitude, though it shifts from negative to positive with depth in general, indicating that the water made more dense in the shallower layer is transported downward. The highest formation rate of 170 m^3/day is found in the lowest layer, and the overall formation rate in the whole CG is also nearly zero (-1.1×10^{-11} m^3/day). The role of cabbeling mixing here is to change the potential energy, rather than to effect the downward transport of water, as in AFZ.

The mixing in WG is the most variable of all the frontal areas. The significant cabbeling area is confined to waters below $\gamma 28.0$ and the mixing takes place in a limited density range. However, its vertical distribution varies from 200 m to 1000 m and the mixing property is highly variable with different source waters (Fig. 12d). mNAW, AIW and DW are adjacent in the spatial domain and cabbeling mixing occurs between these source waters at different depths accompanying high pressure gradient in some areas. Mixing in the upper neutral layers occurs between mNAW and AIW or within mNAW and below mNAW, the mixing occurs between AIW and DW or within DW. The maximum formation rate is found in the lowest layer where the densest water, DW, is formed at the rate of 115 m^3/day. The positive formation rate at $\gamma 28.0$ corresponds to the mixing of mNAW whereas that at $\gamma 28.05 \sim \gamma 28.07$ is due to the mixing between AIW and DW. The overall formation rate in WG is nearly zero (-8.2×10^{-11} m^3/day) indicating that the downward transport across the upper layer ($<\gamma 28.0$) is compensated by the water production in the lower layers (>γ28.0).

The downward transport by cabbeling mixing in SB is remarkable and it increases NAW volume, whereas the role of cabbeling mixing in the other frontal areas is to change buoyancy, and thus would contribute to preconditioning for winter convection. The mixing in WG occurs in the intermediate layer, indicating that the cabbeling mixing has a direct connection to the deeper layer below the permanent pycnocline.

4.3 Density gain due to cabbeling process

A bulk buoyancy change in each frontal area is quantified by estimating the deviation of mixed water density from the average density of source waters. The density anomaly is calculated using in situ density and its dianeutral profiles in each frontal area are shown in Fig. 13. The density anomaly in SB increases towards γ27.62, with the net in situ density gain of 7.6×10^{-3} kg/m^3, and it decreases nearly to half of the maximum anomaly. The upper part of the density anomaly in SB is the greatest found over all frontal areas. The increase of density anomaly above γ27.62 is consistent with the increase of cabbeling-induced velocity. In the lower layer, however, the linear relation between density anomaly and velocity is less obvious. Compared to the water formation rate, it is seen that the highest density anomaly appears in the uppermost layers of positive formation rate. The high density anomaly causes high downward velocity and the cabbeling-produced water is accumulated in the layers of positive formation rate in which in situ density of the cabbeling-induced water is close to that of the surroundings. The density gain as a whole is obtained by density anomaly averaged over whole frontal space. In situ density is not conserved in space, therefore, the deviation in potential density referenced to surface is calculated and the results are listed in Table 4. The density gain in SB as a whole is 3.0×10^{-3} kg/m^3.

In AFZ, the density anomaly in NAW mixing area (above γ27.90) is slightly higher than that in mNAW mixing area (below γ27.90), though the difference is small. The cabbeling-induced velocity, on the other hand, is lower in NAW mixing area than in mNAW mixing area. This is because higher stratification above γ27.90 prevents the generation of downward velocity and it requires a higher density anomaly to make a water parcel sink. The highest density anomaly in NAW mixing area appears at $\gamma 27.83$, which the first positive formation layer, with 2×10^{-3} kg/m^3 whereas that in the mNAW mixing area is more homogeneous with 1.0×10^{-3} kg/m^3 and there is no clear consistency with the formation rate. The overall density gain in AFZ is 1.0×10^{-3} kg/m^3.

The density anomaly in CG decreases with depth, from 2.5×10^{-3} kg/m^3 at $\gamma 27.97$ to 0.5×10^{-3} kg/m^3 at $\gamma 28.03$, and it agrees in general with the distribution of the water formation rate, which increases from negative to positive with depth. The density gain in CG as a whole is the same as that in AFZ.

In WG the density anomaly is the highest (1.0×10^{-3} kg/m^3) in the uppermost layer at $\gamma 28.0$, and density anomaly below is one order lower. There is a minor maximum at $\gamma 28.04$, which corresponds to velocity maximum. The velocity magnitude and density anomaly tends to have a linear correlation, though it is not straightforward where the buoyancy is almost neutral. The density gain in whole WG area is 1.0×10^{-3} kg/m^3.

The overall density gain in AFZ, CG and WG is the same, though the area of these fronts varies as shown in Table 3. The whole spatial area of the analysis domain is 1.17×10^9 m^2 and the areal percentage for each front is 8.2%, 5.2%, 5.0% and 32.3% for SB, AFZ, CG and WG respectively. The densification in the fronts estimated from net density gain times areal will be 2.5×10^{-4} kg/m^3, 5.2×10^{-5} kg/m^3, 5.0×10^{-5} kg/m^3 and 3.2×10^{-4} kg/m^3. The contribution of WG to decrease buoyancy in the Greenland Basin is the highest. The frontal areas occupied approximately 50 % of the whole analysis area and the total density gain in the Greenland Basin due to cabbeling process was estimated as 6.7×10^{-4} kg/m^3.

5 Concluding remarks

The four active cabbeling areas have different characteristics. SB is the area of the most vigorous mixing accompanied by the highest vertical velocity. The transformation of BIW to NAW is the driving force. AFZ has two mixing regimes; mixing within NAW

OSD
5, 507–543, 2008
Cabbeling in the Greenland Basin
Y. Kasajima and T. Johannessen

in the eastern, shallow area and mixing of mNAW and AIW in the western, deeper area. The deeper mixing appears stronger than the shallower mixing. The strength of mixing in CG is equivalent to that of the deeper mixing in AFZ and the resultant water is mNAW. The mixing in WG is the most variable with three source waters in the depth range 200∼1000 m, which covers the whole intermediate layer and partly at the permanent pycnocline. Due to its large space and the formation of the densest water in all four areas, cabbeling mixing in WG has the largest impact on densification of the Greenland Sea water even though each mixing is weak and mixing points are widely separated.

In addition to characteristics described above, the strong cabbeling-induced velocity in SB has a potential to establish a carbon sink. The active cabbeling spots in SB form a columnar structure that may act as a transport pipe, transporting the surface water to the bottom. The water in the Barents Sea is rich in inorganic carbon (Omar et al., 2006) and the conversion of BIW in Barents Sea Opening may transport high $p\mathrm{CO}_2$ water into the deep Greenland Basin.

In the deep part of WG, the product water is classified as DW in some mixing spots. DW and other waters comprising 30% of the total volume (see Table 2) determine the overall density of the Greenland Basin, and hence the volume increase of these dense waters contributes directly to maintain the density contrast between the Greenland Basin and the surrounding basins. At the intermediate layer, the inflow of the re-circulated NAW is substantial for significant cabbeling. The study area belongs to β-oceans (Carmack, 2007) where density change is more sensitive to salinity than to temperature, and the strength of the re-circulated NAW can affect the cabbeling impact on densification in the western Greenland Sea. Salinity of the re-circulated NAW in 2006 reaches 35, which is equivalent to that of NAW in the eastern Greenland Sea, and cabbeling in WG is stronger than in Arctic Frontal Zone in the east.

Acknowledgements. We appreciate the financial support from the EU through IP CARBOOCEAN (contract 511176-2) and the Norwegian Research Council through the International Polar Year project, iAOOS-Norway. We thank to I. Fer and P. M. Haugan for comments on earlier

OSD

5, 507–543, 2008

Cabbeling in the Greenland Basin

Y. Kasajima and T. Johannessen

versions of the manuscript.

References

Akitomo, K.: Open-ocean deep convection due to thermobaricity 1. Scaling argument, J. Geophys, Res., 104(C3), 5225–5234, 1999.

Bönisch, G., Blindheim, J., Bullister, J., Schlosser, P., and Wallace, D.: Long-term trends of temperature, salinity, density and transient tracers in the central Greenland Sea, J. Geophys. Res., 102, 18 553–18 571, 1997.

Budéus, G., Schneider, W., and Krause, G.: Winter convective events and bottom water warming in the Greenland Sea, J. Geophys. Res., 103(C9), 18 513–18 527, 1998.

Carmack, E. C.: The alph/beta ocean distinction: A perspective on freshwater fluxes, convection, nuitrients and productivity in high-latitude seas. Deep-Sea Res., part2, 54, 2579–2598, 2007.

Clarke, R., Swift, J., Reid, J., and Kolterman, K. : The formation f Greelnad Sea Deep Water: Double Diffusion or deep convection?, Deep Sea Res. Part A, 37, 1385–1424, 1990.

Cottier, F. R. and Venables, E. J.: On the double-diffusive and cabbeling environment of the Arctic Front, West Spitsbergen, Polar Res., 26, 152–159, 2007.

Garrett, C and Horne, E. : Frontal circulation due to cabbeling and Double diffusion, J. Geophys. Res., 83(C9), 4651–4656, 1978.

Gill, A. E.: Atmosphere-ocean dynamics, Academic Press, 1982.

Gordon, A. L., Georgi, D. T., and Taylor, H. W.: Antarctic polar front zone in the western Scotia Sea, J. Phys. Oceanogr., 7, 309–328, 1977.

Hansen, B. and Østerhus, S.: North Atlantic-Nordic Seas exchanges, Prog. in Oceanography, 45, 109–208, 2000.

Horne, E. P.W.: Interleaving at the subsurface front in the slope water off Nova Scotia, J. Geophys. Res., 83, 3659–3671, 1978.

Jansen, E and Opheim, V.: European Subpolar Ocean Program (ESOP-II) The thermohaline circulation in the Greenland Sea-Final scientific report, contract MAS3-CT95-0015, Eur. Union, Brussels, 1999.

Karstensen, J., Schlosser, P., Wallace, D. W. R., Bullister, J. L., and Blindeheim, J.: Water mass

transformation in the Greenland Sea during the 1990s, J. Geophys. Res., 110, C07002, doi:10.1029/2004JC002510, 2005.
Loeng, H.: Features of the physical oceanographi conditions of the Barents Sea. Polar Res., 10, 5–18, 1990.
Marsh, R.: Cabbeling due to isopycnal mixing in isopycnic coordinate models, J. Phys. Oceanogr., 30, 1757–1775, 2000.
McDougall, T. J.: Thermobaricity, cabbeling and water mass conversion, J. Geophys. Res., 92(C5), 5448–5464, 1987a.
McDougall, T. J.: Neutral surface. J. Phys. Oceanogr., 17, 1950–1964, 1987b.
McDougall, T. J.: The relative roles of diapycnal and isopycnal mixing on subsurface water mass conversion, J. Phys. Oceanogr. 14, 1577–1589, 1984.
Messias, M.-J., Watson, A. T., Johannessen, T., Oliver, K. I. C., Olsson, K. A., Fogelqvist, E., Olafsson, J., Bacaon, S., Balle, J., Balle, N., Bergman, N., Budéus, G., Danielsen, M., Gascard, J.-C., Jeansson, E., Olafsdottir, S. R., Simonsen, K., Tauhua, T., Van Scoy, K., and Ledwell, J. R.: The Greenland Sea Tracer Experiment 1996-2002: horizontal mixing and transport of Greenland Sea Intermediate Water, Progress in Oceanography, 78, 85–105, doi10.1016/j.pocean.2007.06.005, 2007.
Munk, W. H. and Wunch, C.: Abyssal Recipes II: energetics of tidal and wind mixing, Deep-Sea Res., 45, 1977–2010, 1998.
Omar, A., Johannessen, T., Kaltin, S., and Olsen, A.: Anthropogenic increase of oceanic $p\mathrm{CO}_2$ in the Barents Sea surface water, J. Geophys. Res., 108(C12), 388, doi:10.1029/2002JC001628, 2003.
Sundfjord, A. Fer, I., Kasajima, Y., and Svendsen, H.: Observations of turbulent mixing and hydrography in the marginal ice zone of the Barents Sea, J. Geophys. Res., 112, C05008, doi:101029/2006JC003524, 2007.
Swift, J. H. and Aagaard, K.: Seasonal transitions and water mass formation in the Iceland and Greenland seas, Deep-Sea Res., 28(A10), 1107–1129, 1981.
Talley, L. and Yun, J. Y.: Role of cabbeling and double diffusion in setting the density of the North Pacific intermediate water salinity minimum, J. Phys.Oceanogr., 31, 1538–1549, 2001.
van Aken, H., Budéus, G., and Hahnel, M.: The anatomy of the Arctic Frontal Zone in the Greenland Sea, J. Geophys. Res., 100(C8), 15 999–16 014, 1995.
van Aken, H. M., Quadfasel, D., and Warpakowski, A.: The Arctic front in the Greenland Sea during February 1989: Hydrographyc and biological observations, J. Geophys. Res,. 96,

OSD
5, 507–543, 2008

Cabbeling in the Greenland Basin

Y. Kasajima and T. Johannessen

4739–4750, 1991.
Walin, G.: On the relation between sea-surface heat flow and thermal circulation in the ocean, Tellus, 34, 187–195, 1982.
You, Y.: Dianeutral mixing in the thermocline of the Indian Ocean, Deep-Sea Res. Part I, 43, 291–320, 1996.
You, Y.: Dianeutral mixing, transformation and transformation and transport of Antarctic Intermediate Water in the South Atlantic Ocean, Deep-Sea Res. Part II, 46, 393–435, 1999.

Table 1. Water mass classification in the Greenland and Iceland Seas according to Swift and Aagaard (1981); AW, PW, uAIW, lAIW, NSDW, GSDW, van Aken et al. (1995); NwAW, AW type, Loeng (1990); SBW.

Water type	Salinity	θ
Atlantic Water (AW)	35.1<S 35.3	$6<\theta<8$
Norwegian Atlantic Water (NwAW)	35.0<S	$3<\theta$
AW type	34.9<S	$2<\theta$
Polar Water (PW)	33.0<S<34.4	$3<\theta<5$
Upper Arctic Intermediate Water (uAIW)	34.9<S<35.0	$0<\theta<3$
Lower Arctic Intermediate Water (lAIW)	34.7<S<34.9	$\theta<2$
Norwegian Sea Deep Water (NSDW)	34.90<S<34.94	$\theta<0$
Greenland Sea Deep Water (GSDW)	34.88<S<34.90	$\theta<-1$
Spitsbergen Bank Water (SBW)	S<34.4	$1<\theta<3$

OSD

5, 507–543, 2008

Table 2. Water types found in the current dataset. The relative volume percentage is calculated by data points which satisfy the salinity temperature range for water types devided by the total data number times 100.

Water type	Salinity	Potential temperature	Relative volume percentage
Norwegian Atlantic Water (NAW)	34.9<S	$3<\theta$	5.8%
Modified Atlantic Water (mNAW)	34.9<S	$0<\theta<3$	7.5%
Arctic Intermediate Water (AIW)	34.7<S<34.9	$\theta<2$	1.9%
Dense Water (DW)	34.90<S<34.94	$\theta<0$	53.4%
Bear Island Water (BIW)	S<34.9	$3<\theta$	0.71%

OSD
5, 507–543, 2008

Table 3. The area of high cabbeling mixing. SB corresponds to Polar Front, AFZb–c are in the Arctic Frontal Zone, CG locates in the central Greenland Sea, WG1–2 are at the western boundary of the Greenland Sea gyre.

Name	Spatial distribution	Depth variation	Front waters	Vertical expansion ($\times 10^7$ m^2)
SB	16.5–18.5 E	13–205 m	BIW, NAW	9.5996
AFZ				
AFZc	8–8.5 E	62–245 m	NAW	2.3140
AFZb	5–7.5 E	51–302 m	NAW, mNAW and AIW	3.6354
CG	5–3 W	41–210 m	mNAW and AIW	5.8500
WG				
WG1	9.3–7 W	78–700 m	mNAW and AIW	19.3644
WG2	12–10 W	221–1152 m	mNAW and AIW	18.3864

OSD

5, 507–543, 2008

Cabbeling in the Greenland Basin

Y. Kasajima and T. Johannessen

Table 4. Density of parent waters and the mixed water at each frontal area.

Front		σ_θ	density increase (kg/m^3)
SB	Mixed water	27.615	0.003
	Source water averaged	27.611	
AFZ	mixed water	27.867	0.001
	Source water averaged	27.866	
CG	mixed water	27.984	0.001
	Source water averaged	27.983	
WG	mixed water	28.031	0.001
	Source water averaged	28.030	

OSD
5, 507–543, 2008

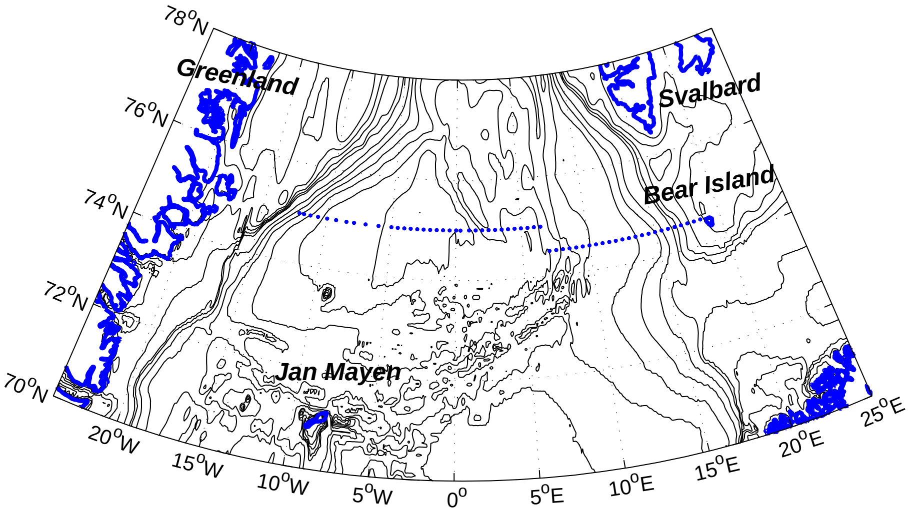

Fig. 1. CTD stations in the study area.

OSD

5, 507–543, 2008

Cabbeling in the Greenland Basin

Y. Kasajima and T. Johannessen

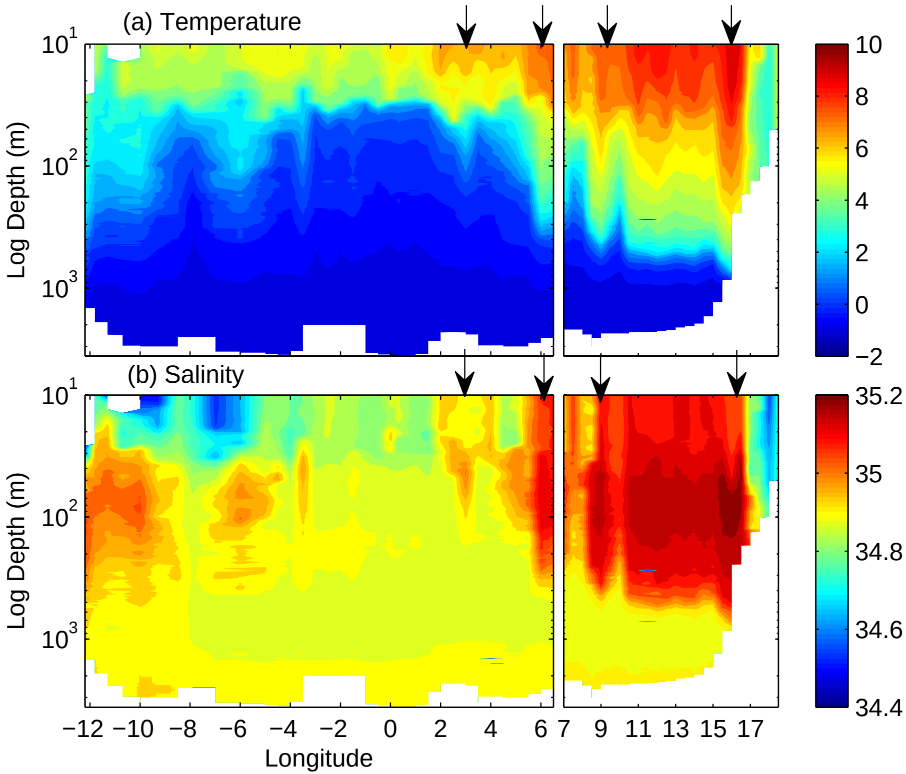

Fig. 2. **(a)** Temperature and **(b)** salinity across the Greenland Basin. The arrows indicate the frontal interfaces according to van Aken et al. (1991).

5, 507–543, 2008

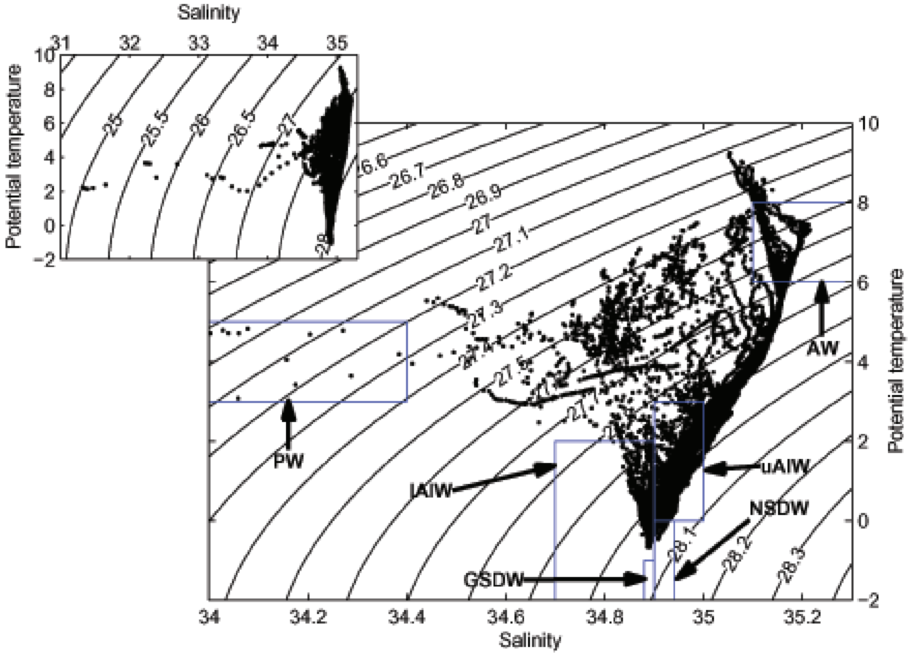

Fig. 3. T-S diagram for all data points (upper small diagram) and for more focused data points (large diagram). Water types defined by Swift and Aagaard (1981) are indicated with boxes in the large diagram.

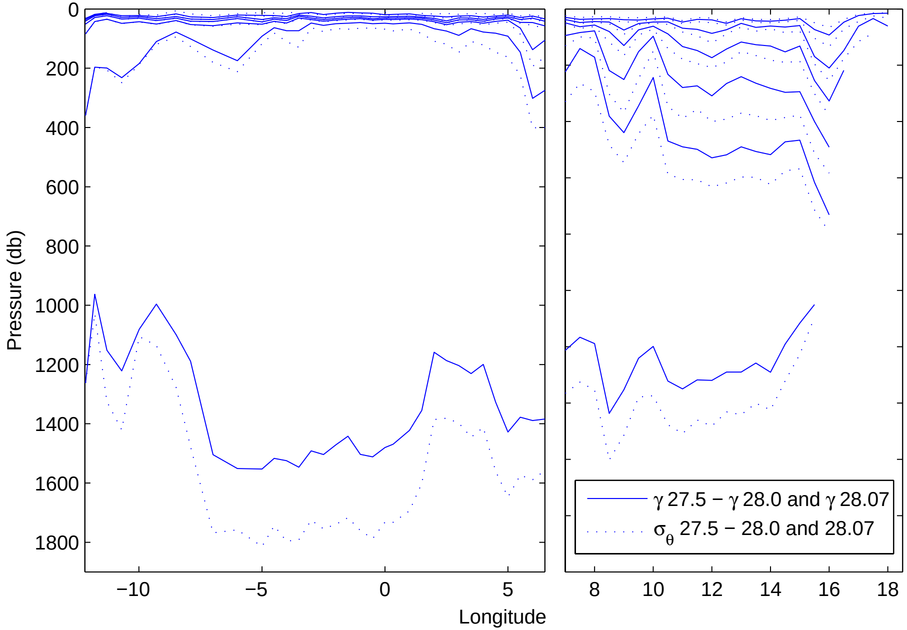

Fig. 4. Neutral surfaces (solid lines) and isopycnals referenced to surface (dotted lines) across the Greenland Basin. Lines display 27.5, 27.6, 27.7, 27.8, 27.9, 28.0 and 28.07 from the shallow water. The shallowest neutral surface, γ27.5, outcrops and it is not appeared in the east of 10.7° W.

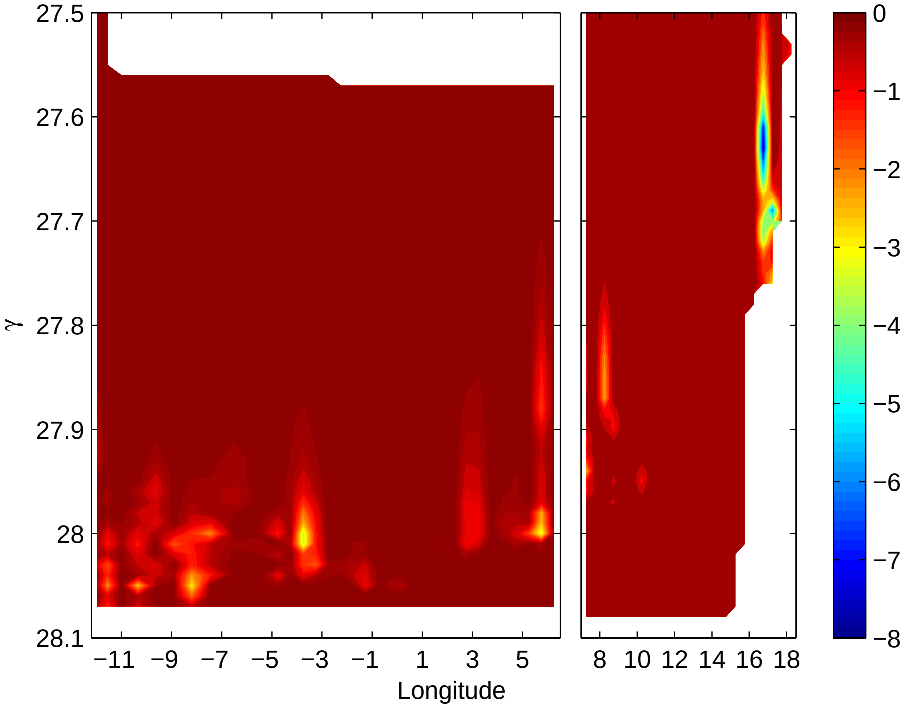

Fig. 5. Cabbeling-induced velocity in the neutral surface domain (m/day).

OSD

5, 507–543, 2008

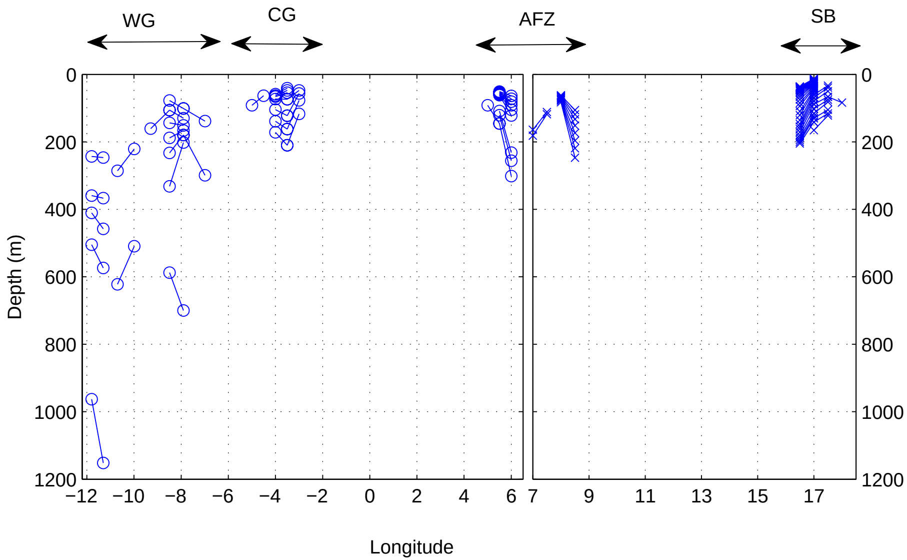

Fig. 6. Active cabbeling mixing areas in pressure-longitude domain. Mixing which generates velocities greater than 1 m/day is shown with its source water locations connected with a line. The mixing areas are distinguished as SB, AFZ, CG and WG as indicated on the top.

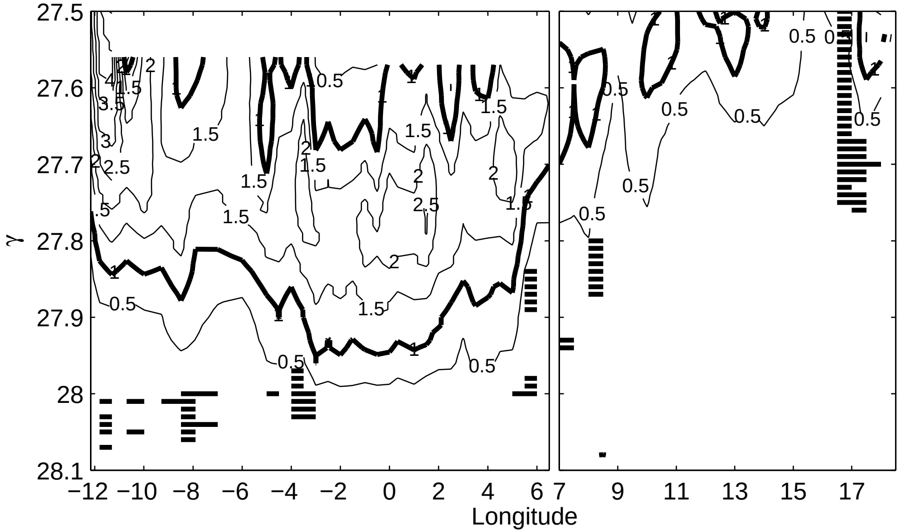

Fig. 7. Bouyancy frequency ($\times 10^{-4}$ s^{-1}) and the areas in which cabbeling-induced velocity is more than 1 m/day. The thick lines indicate N^2=1.0×10^{-4}.

OSD

5, 507–543, 2008

Cabbeling in the Greenland Basin

Y. Kasajima and T. Johannessen

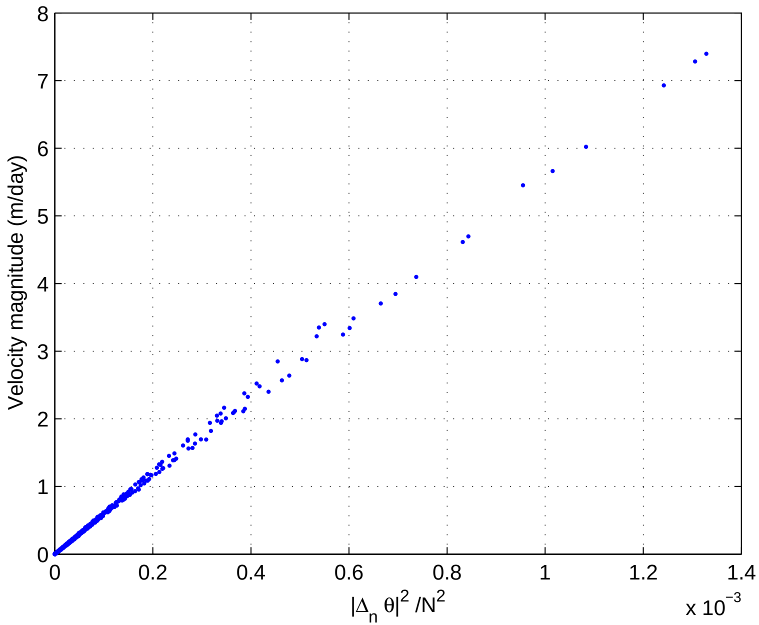

Fig. 8. The relation between the temperature gradient to stratification ratio and velocity.

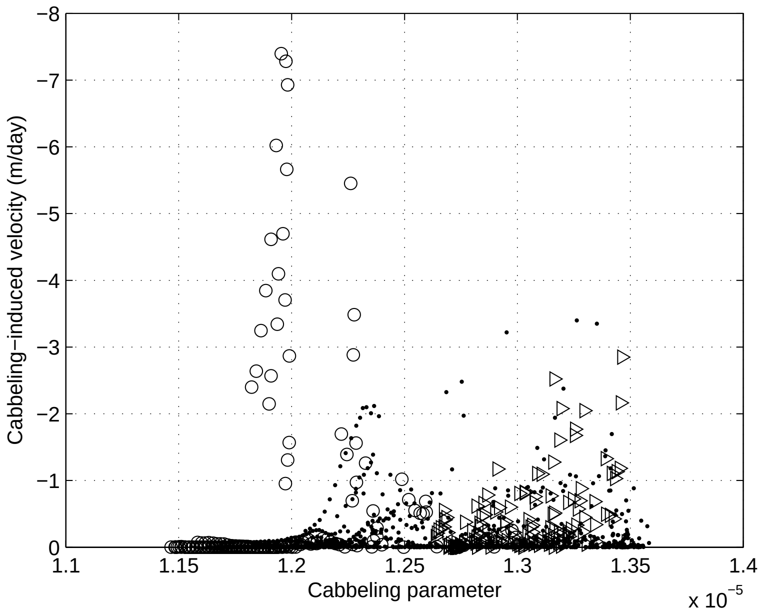

Fig. 9. The relation between cabbeling-induced velocity and the cabbeling parameter. Circles are from the area east of 9° E, triangles are from west of 7° W and dots are from the area between them.

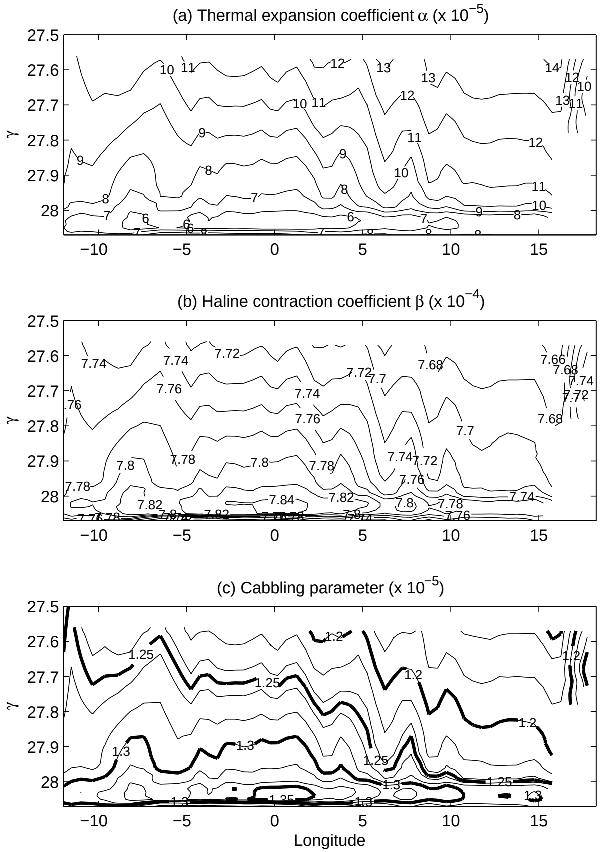

Fig. 10. **(a)** Thermal expansion coefficient, α, **(b)** haline contraction coefficient, β, and **(c)** cabbeling parameter.

OSD
5, 507–543, 2008

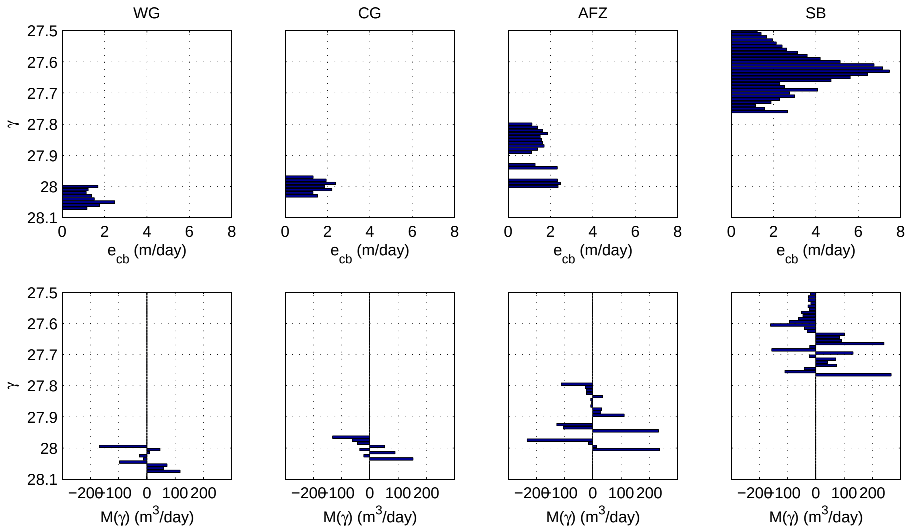

Fig. 11. Velocity averaged over surfaces at fixed γ (m/day) and water formation rate (m^3/day).

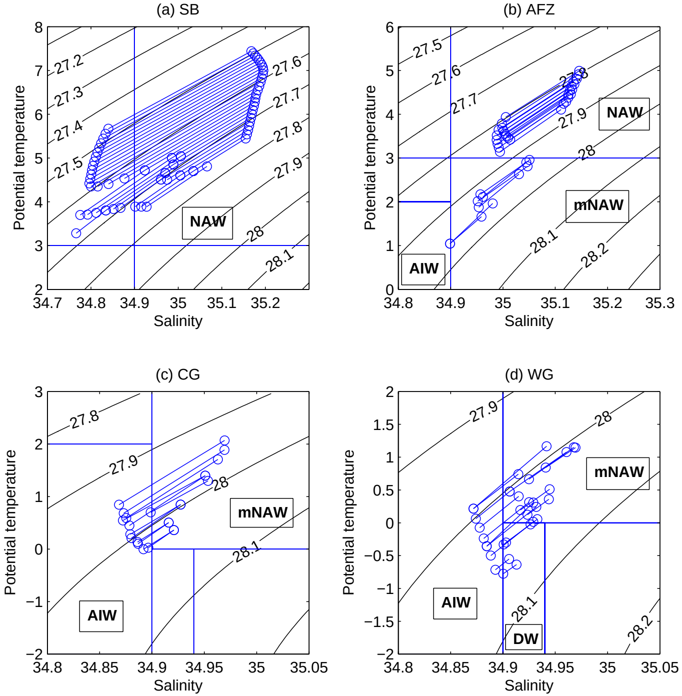

Fig. 12. T-S diagrams of mixing source water in **(a)** SB, **(b)** AFZ, **(c)** CG and **(d)** WG. Two end-members are connected with a line and the mixed water property is assumed to be in the middle of the line.

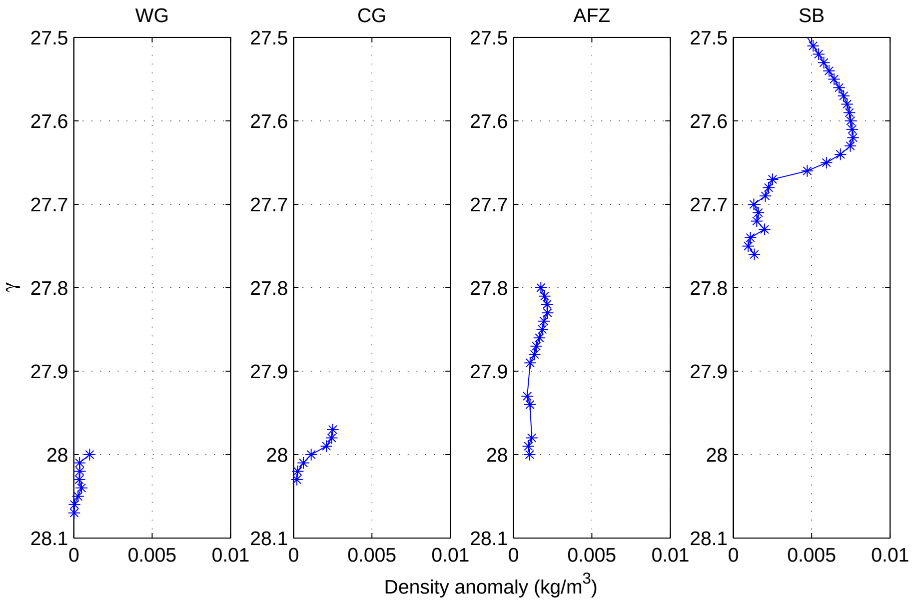

Fig. 13. Density anomaly estimated from the difference between averaged density of source water and density of the mixed water.

OSD
5, 507–543, 2008

Cabbeling in the Greenland Basin

Y. Kasajima and T. Johannessen